Magnetic Resonance Imaging 61 (2019) 149–157

Contents lists available at ScienceDirect

Magnetic Resonance Imaging

journal homepage: www.elsevier.com/locate/mri

Original contribution

Simultaneous R2, R2' and R2* measurement of skeletal muscle in a rabbit model of unilateral artery embolization

Yao Wang[a], Rui Zhang[b], Bihui Zhang[c], Chengyan Wang[a], Haochen Wang[c], Xiaodong Zhang[d], Kai Zhao[d], Min Yang[c], Xiaoying Wang[a,d,*], Jue Zhang[a,b,**]

[a] Academy for Advanced Interdisciplinary Studies, Peking University, Beijing, China
[b] College of Engineering, Peking University, Beijing, China
[c] Department of Interventional Vascular Surgery, Peking University First Hospital, Beijing, China
[d] Department of Radiology, Peking University First Hospital, Beijing, China

ARTICLE INFO

Keywords:
Unilateral artery embolization model
Simultaneous measurement
The MEGSE sequence
R2
R2' and R2*
Sensitivity
Feasibility

ABSTRACT

Purpose: To demonstrate the feasibility of using a susceptibility-based MRI technique with multi-echo gradient and spin echo (MEGSE) sequence to achieve simultaneous R2, R2' and R2* measurement and assess skeletal muscle oxygenation alternations in a rabbit model of unilateral artery embolization.

Materials and Methods: Approved by the local institutional review board for experimental animal studies, nine New Zealand White rabbits were included in this study. The MEGSE sequence consists of embedding a set of gradient echoes around the echo of a single spin-echo sequence using several gradient echoes to collect the magnetization intensity during the formation and attenuation of spin-echo simultaneously after 180° radio frequency pulse. Within-session and between-day tests were conducted to evaluate the reproducibility of this skeletal muscle oxygenation alternations measurement. Furthermore, all the MEGSE scans of skeletal muscle were conducted using a 3-T clinical MRI scanner during resting state (before unilateral artery embolization operation, pre), 1 h after unilateral artery embolization operation (post1) and 2 h after unilateral artery embolization operation (post2) model to verify the feasibility and sensitivity of this method.

Results: The within-session coefficient of variations (CVs) of R2, R2' and R2* measurements were 1.57%, 3.33% and 2.57%, while the between-day CVs of were 1.42%, 5.85% and 2.85%. In all rabbits, the mean R2 decreased significantly from 36.46 ± 1.03 s^{-1} (pre) to 30.58 ± 2.11 s^{-1} (post1,**P < 0.01, relative to pre) and 28.62 ± 1.53 s^{-1} (post2, **P < 0.01, relative to post1), and the mean R2' went up markedly from 9.88 ± 2.14 s^{-1} (pre) to 16.10 ± 2.74 s^{-1} (post1, **P < 0.01) and 17.33 ± 2.25 s^{-1} (post2, **P < 0.05). The mean R2* increased from 43.27 ± 3.75 s^{-1} (pre) to 47.90 ± 5.08 s^{-1} (post1, *P < 0.05) and to 48.04 ± 4.42 s^{-1} (post2, NS, P > 0.05).

Conclusion: This study demonstrates the feasibility of simultaneous R2, R2' and R2* measurement method for the evaluation of skeletal muscle ischemia. Besides, this study indicates the sensitivity of the R2 and R2' compared with R2* and especially the necessity of R2 and R2' measurement for the further evaluation of skeletal muscle ischemia which always causes both edema and hypoxia in a rabbit model of unilateral artery embolization.

1. Introduction

The incidence of limb arterial ischemic diseases, especially the lower extremity arterial ischemic diseases, is increasing year by year and has gradually become one of the leading causes of death and disability in the elderly. The incidence in adults is about 12%, while the incidence among the age of 70 or above is up to 20% [1]. Especially for patients with diabetes and hypertension, 20% to 50% of them have the possibility of lower extremity arterial ischemic disease [2].

Meanwhile, skeletal muscle ischemia often indicates vascular

* Correspondence to: X. Wang, Academy for Advanced Interdisciplinary Studies, Peking University, Beijing, China. Department of Radiology, Peking University First Hospital, Beijing, China
** Correspondence to: J. Zhang, Academy for Advanced Interdisciplinary Studies, Peking University, Beijing, China. College of Engineering, Peking University, Beijing, China
E-mail addresses: cjr.wangxiaoying@vip.163.com (X. Wang), zhangjue@pku.edu.cn (J. Zhang).

https://doi.org/10.1016/j.mri.2019.05.030
Received 31 August 2018; Received in revised form 20 May 2019; Accepted 20 May 2019

surgery. The severity and the development of the disease are closely related to the arterial stenosis, the compensatory ability of collateral circulation after occlusion and the changes in oxygen metabolism [3].Therefore, the quantitative measurements of oxygen metabolism in ischemia lower limbs and foot tissues also have practical significance [4].

Many methods have been proposed and applied in the characterization of muscle oxygen consumption. Commonly, transcutaneous oxygen pressure (TcPO2) with modified Clark electrodes [5] used for estimating the tissue oxygenation in lower limbs to evaluate the degree of ischemia in clinical diagnosis. However, this technique can only detect the skin microvasculature, and only indirectly represents oxygen condition of muscle. Recently, near-infrared spectroscopy (NIRS) and positron emission tomography (PET) have been adopted to measure regional skeletal muscle oxygen consumption. However, the oxygen condition of deep muscle tissue cannot be acquired by NIRS due to its limited penetration capacity. Moreover, the radioactive isotopes injection, poor spatiotemporal resolution, and ionizing radiation of PET constrain its broad application in the skeletal muscle oxygenation investigation [6,7]. Clinically, the invasive microelectrode technique has also been applied to evaluate muscle oxygenation, but it suffers from the problem of poor spatiotemporal resolution except for the invasive treatment.

Due to the advantages of deep penetration, nonionizing radiation, and high spatial resolution, MRI has been widely applied in the study of skeletal muscle oxygen consumption and metabolism [8]. Previous studies have adequately demonstrated the effectiveness of the evaluation skeletal muscle oxygen metabolism using BOLD technique [9].BOLD technology focuses on R2* and signal changes in the corresponding T2* weighted images. Specifically, the effective transverse relaxation rate $R_2^*(=1/T_2^*)$ is equal to $R_2 + R_2'$, where R_2 $(=1/T_2)$ represents the intrinsic relaxation rate and R_2' $(=1/T_2')$ stands for the reversible contribution to the total relaxation time. R2 used to characterize pathological changes caused by tissue edema and inflammation [10,11]. R2' is more appropriate for the characterization of magnetic susceptibility [12] and R2' can evaluate skeletal muscle oxygen consumption. These methods are also of great importance for the evaluation of skeletal muscle blood vessels circulation and the diagnosis of limb vascular disease.

Interestingly, we found some studies [13–15] used the relative change ratio of R2 and R2 * (R2/R2*) as an indicator to assess the size of vessels. Further, R2 and R2* imaging information can quantify the average size of brain vessels [16,17]. These methods are also essential for evaluating the vascular circulatory function of skeletal muscle and the diagnosis of vascular diseases of limbs. More and more researchers hope to obtain R2 and R2' in R2* respectively to better evaluate the oxygen metabolism of skeletal muscle. Inspired by the results above, we think it is necessary to obtain accurate quantitative information of R2, R2', R2*, not just R2*.

Traditionally, R_2 can be derived from the multi-echo spin-echo (MSE) method, while R_2^* can be measured by the multi-echo gradient-echo (MGE) approach [12]. Elder [18] utilized dual gradient-echo (GE) echo-planar imaging (EPI) and dual spin-echo (SE) EPI sequences to obtain R2' (R2' = R2* − R2) value and established an empirical relationship between ΔR2' and NIRS observed oxyhemoglobin saturation under cuff compression condition. However, two separate scans are needed, and the physiological variability and position changes between these two separated imaging scans exist. In addition, this method also causes EPI artifacts. A sequence with an efficient quantification of R_2, R_2' and R_2^* simultaneously would be valuable. Ma [19] have proposed a gradient echo sampling of the free induction decay (FID) and echo (GESFIDE) sequence, which can acquire R_2 and R_2^* simultaneously combined with a single exponential model. Similar to GESFIDE sequence, recently, a multiple spin- and gradient-echo (SAGE) sequence with echo-planar imaging (EPI) acquisition scheme was proposed which allowed simultaneous quantification of R_2 and R_2^* during a dynamic event [20–22]. However, due to the non-ideal slice profile caused by short RF pulse duration, the GESFIDE and SAGE methods suffer a problem of slice profile mismatch between images prior to and after the 180° refocusing pulse, which results in certain estimation errors in estimating R_2 and R_2^*.

From this perspective, the multi-echo gradient and spin echo (MEGSE) sequence is only acquired after the 180° RF pulse, which avoids the slice profile mismatch caused by the echo acquisition on the 180° sides of the GESFIDE sequence. The MEGSE sequence is to avoid some physiological variability and position changes between two separate imaging scans compared with the MSE and MGE sequence. So MEGSE sequence is also used to acquire R2, R2* [23], and are widely applied to the brain of oxygen metabolism and R2 and R2 * imaging evaluation [24,25].

However, to the best of our knowledge, the simultaneous R2, R2' and R2* measurement to evaluate oxygen metabolism of skeletal muscle after embolization has not been reported yet. Muscle tissue, however, comprises muscle fibers and corresponding blood vessels regularly oriented in a parallel fashion for the purpose of maximal force generation, enhancing this effect, which should result in differences in detected BOLD signal [26,27].

The aim of this experimental study was to achieve simultaneous R2, R2' and R2* measurement and assess skeletal muscle oxygenation on the embolized leg muscle with lower signal-to-noise ratio using the MEGSE sequence. To verify the feasibility of the MEGSE-based simultaneous R2, R2' and R2* measurement approach and the changes of R2, R2', R2* for the evaluation of skeletal muscle oxygenation, rabbit models of unilateral artery embolization were confirmed by the digital subtraction angiography (DSA) imaging.

2. Materials and methods

2.1. Animals

The study was approved by the local institutional review board for experimental animal studies. All experiments were performed in accordance with the guidelines and approval of the animal care and use committee of our research center. Nine New Zealand White rabbits (male; weight range 2.8–3.5 kg) were included in this study.

2.2. Study protocol

During the whole experiments, rabbits were anesthetized with 1% isoflurane delivered by a calibrated vaporizer. Rabbits were positioned supine on the MR and interventional surgery operation table with a close-fitting facemask covering the whole mouth and the nose. A flexible tube was connected to the mask leading to the in-house room air supply with a flow rate of 2.5 L/min.

First, the MR measurements of skeletal muscle were performed during the resting state. Then the rabbits were moved to the interventional surgery operation table to perform the unilateral artery embolization operation of the leg.

For each rabbit, to complete embolization of the vessels in the unilateral leg, a 35-inch vascular interventional guide wire was inserted from the neck blood vessel, then was injected microspheres (Embosphere, Merit, Rockland, MD) with diameters of 200 um to the unilateral vessel at the branch of the common iliac artery.

The digital subtraction angiography (DSA) imaging was then implemented to confirm the success of the unilateral artery embolization model. After the unilateral artery embolization operation, the rabbits were moved to the MR table to collect skeletal muscle MRI data 1 h and 2 h after the unilateral artery embolization model. The corresponding image acquisition scheme is shown in Fig. 1. The three statuses were defined as follows, pre: before unilateral artery embolization operation, post1: 1 h after unilateral artery embolization operation, post2: 2 h after unilateral artery embolization operation.

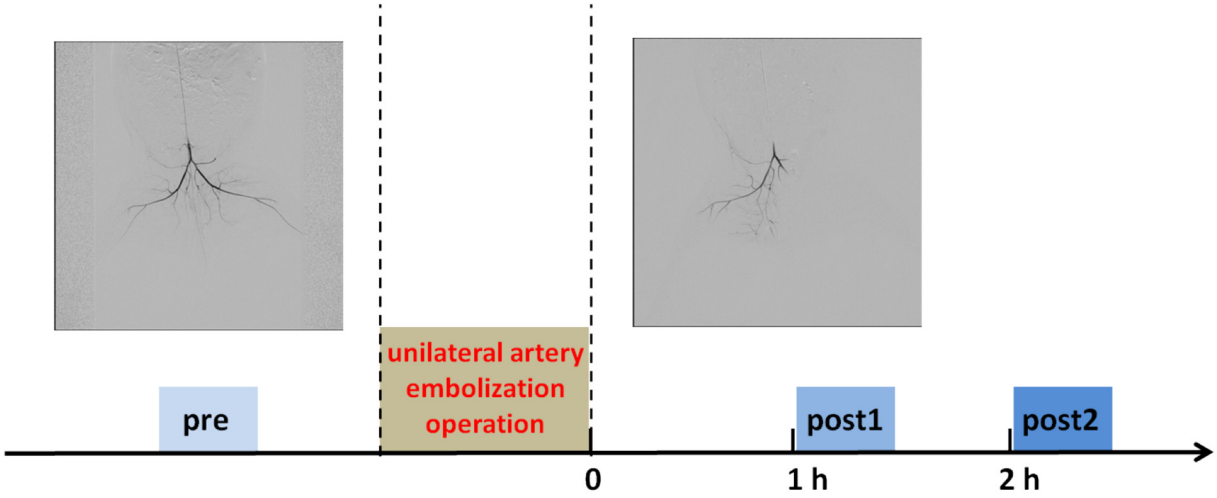

Fig. 1. Imaging scheme of the experiment and digital subtraction angiography imaging results of before and after unilateral leg artery vascular embolization in rabbits. Three statuses are defined as follows: pre: at rest (before unilateral artery embolization operation), post1: 1 h after unilateral artery embolization operation, post2: 2 h after unilateral artery embolization operation.

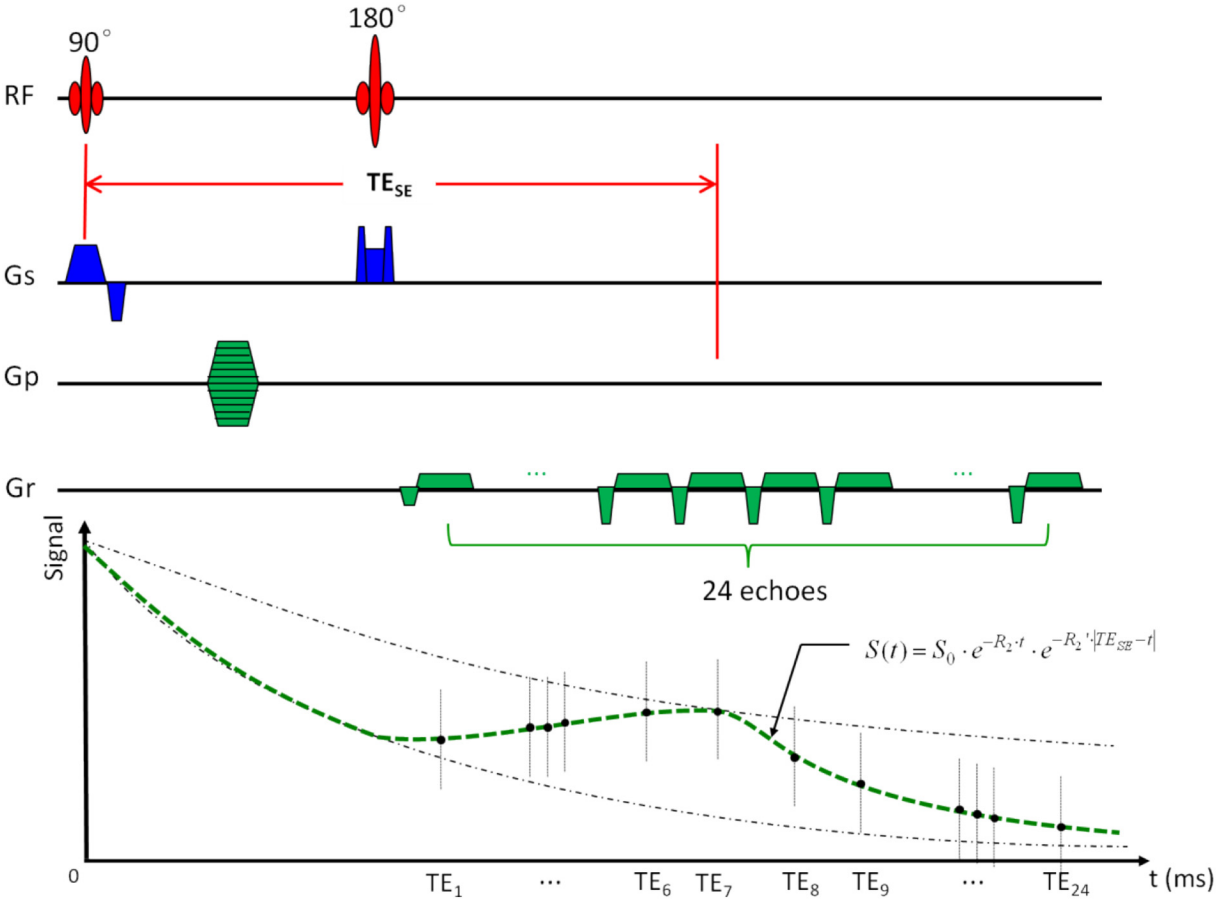

Fig. 2. Schematic diagram of MEGSE sequence and corresponding attenuation curve of echo signal for the calculation of R2, R2' and R2*. The timing parameters are defined in the text. Gs = gradients along the slice-select direction, Gp = gradients along the phase-encoding direction, Gr = gradients along the readout direction.

2.3. MRI data acquisition

All the MRI measurements were carried out on a 3.0-T whole-body MR scanner (Signa ExciteTM; GE Medical System, Milwaukee, Wisconsis, USA). The body coil was used for signal transmission, and an 8-channel knee coil was applied for signal reception.

During each status (pre, post1, post2), axial T2-weighted images of the leg muscle were acquired using a fast spin-echo sequence with field of view (FOV) = 170 × 170 mm^2, repetition time (TR) = 4500 ms, echo time (TE) = 107 ms, slice thickness = 6 mm, matrix size = 256 × 256, echo-train length = 20, number of signals averaged (NSA) = 1.

A two-dimensional, multi-echo gradient and spin echo (MEGSE) sequence (Fig. 2) was used to acquire images and subsequently used to

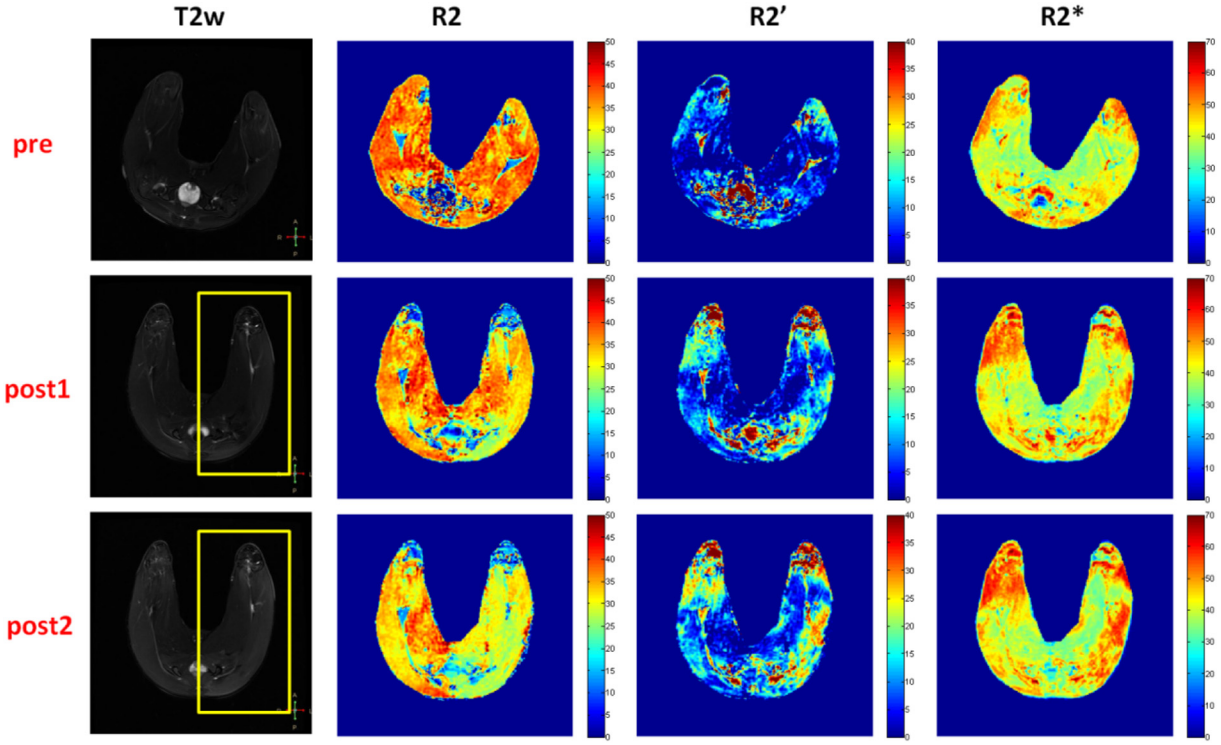

Fig. 3. Representative anatomical T2w image, R2, R2' and R2* maps of leg muscle from one rabbit in the three conditions (pre, post1 and post2). Yellow rectangle region is embolic tissue, which is ROI area. ROI was selected based on T2 weighted images, in which bones and large vessels and their proximal areas were removed. (For interpretation of the references to colour in this figure legend, the reader is referred to the web version of this article.)

Table 1
Baseline within-session and between-day reproducibility results of R2, R2' R2* in rabbit leg muscle (n = 9).

	Scan (mean ± SD)	With-session rescan (mean ± SD)	Between-day rescan (mean ± SD)	With-session CV (%)	Between-day CV (%)
R2 (s^{-1})	36.46 ± 1.03	36.29 ± 1.66	36.26 ± 1.24	1.57%	1.42%
R2' (s^{-1})	9.88 ± 2.14	9.81 ± 2.20	8.96 ± 1.35	3.33%	5.85%
R2* (s^{-1})	43.27 ± 3.75	44.41 ± 2.91	42.63 ± 2.72	2.57%	2.85%

SD = standard deviation, CV = coefficient of variation.

Table 2
The p-values of Shapiro-Wilk test are calculated in both normal and embolization leg muscle (n = 9). Three statuses are as follows: pre: at rest (before unilateral artery embolization operation), post1: 1 h after unilateral artery embolization operation, post2: 2 h after unilateral artery embolization operation.

R2			R2'			R2*		
pre	post1	post2	pre	post1	post2	pre	post1	post2
Normal								
0.280	0.716	0.579	0.356	0.264	0051	0.097	0.952	0.820
Embolization								
0.115	0.785	0.957	0.128	0.162	0.661	0.181	0.749	0.815

Data are P value. P > 005 for all data, it shows that data has normal distribution.

extract R2, R2' and R2*. In total, 24 echoes with an echo spacing (ΔTE) of 2.964 ms were acquired. The spin echo occurred at the seventh echo. The imaging parameters were as follows: TR = 1500 ms, TE = 56 ms, readout bandwidth = 62.5 kHz, acquired matrix = 128 × 128, FOV = 170 × 170 mm^2, slice thickness = 6 mm, and NSA = 1. Although multislice acquisition could be achieved with the MEGSE sequence, only one slice was acquired in this study so that the potential crosstalk, signal interference between two adjacent slices because of an imperfect RF slice profile, could be minimized.

To verify the reproducibility of MEGSE scanning, the normal leg of 9 rabbits with unilateral artery embolization were scanned 3 times in total, twice on the day of embolization (0 min, 20 min) and once the following day (day 1).Then, similar with [28], the coefficient of variation (CV) was used to evaluate the reproducibility during within-session and between-day measurements. To further demonstrate the different influences of unilateral artery embolization model to the normal and ischemia legs, R2, R2' and R2* between normal and ischemia legs were calculated at three statuses (pre, post1, post2), meanwhile the effectiveness of the model was confirmed by DSA imaging after the complete embolization of the unilateral leg blood vessels. The scanning position and protocols stayed the same in all the repetitive measurements.

2.4. Data analysis

Data analysis was performed by using self-developed Matlab (MathWorks Inc., Natick, MA, USA) routines. Before analysis, all the MEGSE images were filtered using a Gaussian low-pass filter (kernel size = 3 × 3) to improve the signal-to-noise ratio (SNR).

In the MEGSE sequence with a specific 180° pulse position, data are subsequently sampled by a multi-echo acquisition scheme with a different offset from the spin echo. In this study, a 24-echo acquisition

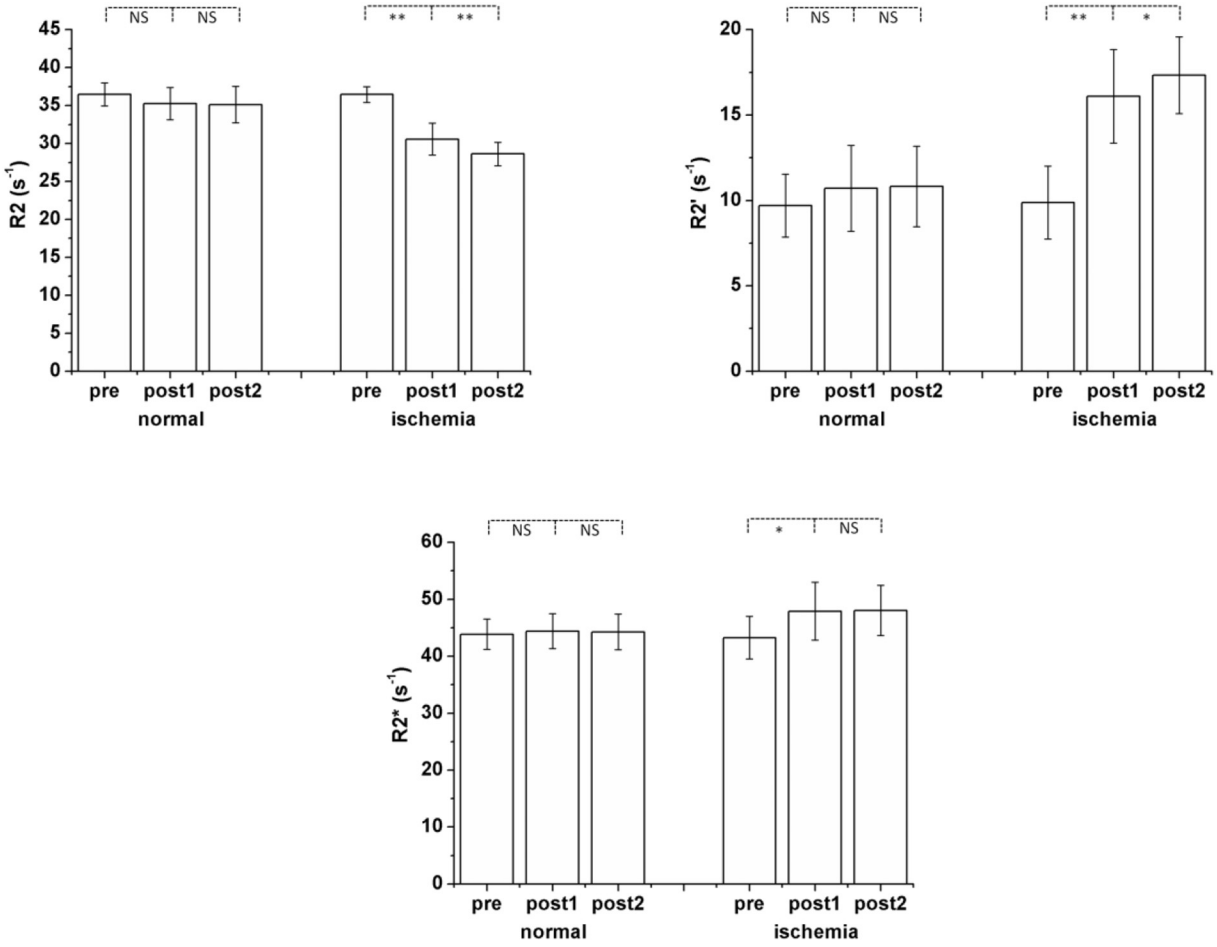

Fig. 4. Average values of R2, R2' and R2* in the left and right leg muscles of all nine rabbits at the three statuses (pre, post1 and post2). *P < 0.05 using paired Student's *t*-test.

scheme is adopted. Echo time (TE_i, i = 1,2, …,24) is defined as the time between the center of the 90° excitation pulse and the *k*-space center of each echo. The echo spacing between two adjacent echoes is defined as ΔTE. Once the first echo data have been acquired, the phase encoding is rewound, and the following twenty-three echo data sets are subsequently acquired identically at TE_2, TE_3, …, TE_{24}, respectively. The magnetization of these data has different contributions of T_2* weighting due to their variable offsets from the spin echo, which is illustrated by the signal evolution curve in Fig. 2. According to a monoexponential decay mode [12,19], the magnitude of the signal as a function of the acquisition time following the 90° pulse is described as follows:

$$S(t) = \begin{cases} S_0 \cdot \exp(-R_2 \cdot t) \cdot \exp[-R_2' \cdot (TE_{SE} - t)], & TE_{SE}/2 < t < TE_{SE} \\ S_0 \cdot \exp(-R_2 \cdot t), & t = TE_{SE} \\ S_0 \cdot \exp(-R_2 \cdot t) \cdot \exp[-R_2' \cdot (t - TE_{SE})], & t > TE_{SE} \end{cases} \quad (1)$$

where S(t) is the magnetization at the acquisition time *t*, S_0 is the magnetization excited by the 90° pulse, and TE_{SE} is the effective echo time where the transverse magnetization is fully refocused by the 180° pulse. This equation can be simplified as follows:

$$S(t) = S_0 \cdot \exp(-R_2 \cdot t) \cdot \exp(-R_2' \cdot |TE_{SE} - t|) \quad (2)$$

By taking the natural logarithm of both sides of Eq. (2), the equation can be written as:

$$\ln(S(t)) = \ln(S_0) - R_2 \cdot t - R_2' \cdot |TE_{SE} - t| \quad (3)$$

R2 can be fitted from the multi-echo image of the symmetric positions on both sides of the spin echo position according to the Eq. (4):

$$R_2 = \ln[S(TE_{SE} - \tau)/S(TE_{SE} + \tau)]/2\tau \quad (4)$$

where τ is the time interval between the corresponding echo position and the spin echo position. A log-linear least-squares curve fitting approach was utilized to obtain R2' by fitting the Eq. (3) on a pixel-by-pixel basis based on the known R2. Finally, the corresponding R2, R2' and R2* maps could be obtained with the fitting processing.

Regions of interest (ROIs) were placed manually in left and right leg muscles. The ROIs were chosen in T2-weighted images to exclude pixels near the bones and large vessels. An example of the ROIs is shown in Fig. 3. Since the scanning position was copied for all the sequences, the same ROI was shared across all the scans.

2.5. Statistical analysis

All the statistical analysis was performed by using Matlab (MathWorks Inc., Natick, MA, USA). Data were reported as mean ± standard deviation.

The reproducibility of the MEGSE sequence was evaluated using the coefficient of variation (CV) [29], which was calculated as the standard deviation divided by the mean value from two different scans.

A paired, two-sided Student *t*-test was applied to assess statistical differences between the two statuses of pre and post1, and also between the two statuses of post1 and post2. Shapiro-Wilk test [30] was made to test the distribution for all measurements prior to analysis, and the measurements are both normally distributed (p > 0.05), as shown in Table 2. A statistically significant difference was considered to be indicated by a P value of < 0.05.

To further demonstrate the different influences of unilateral artery

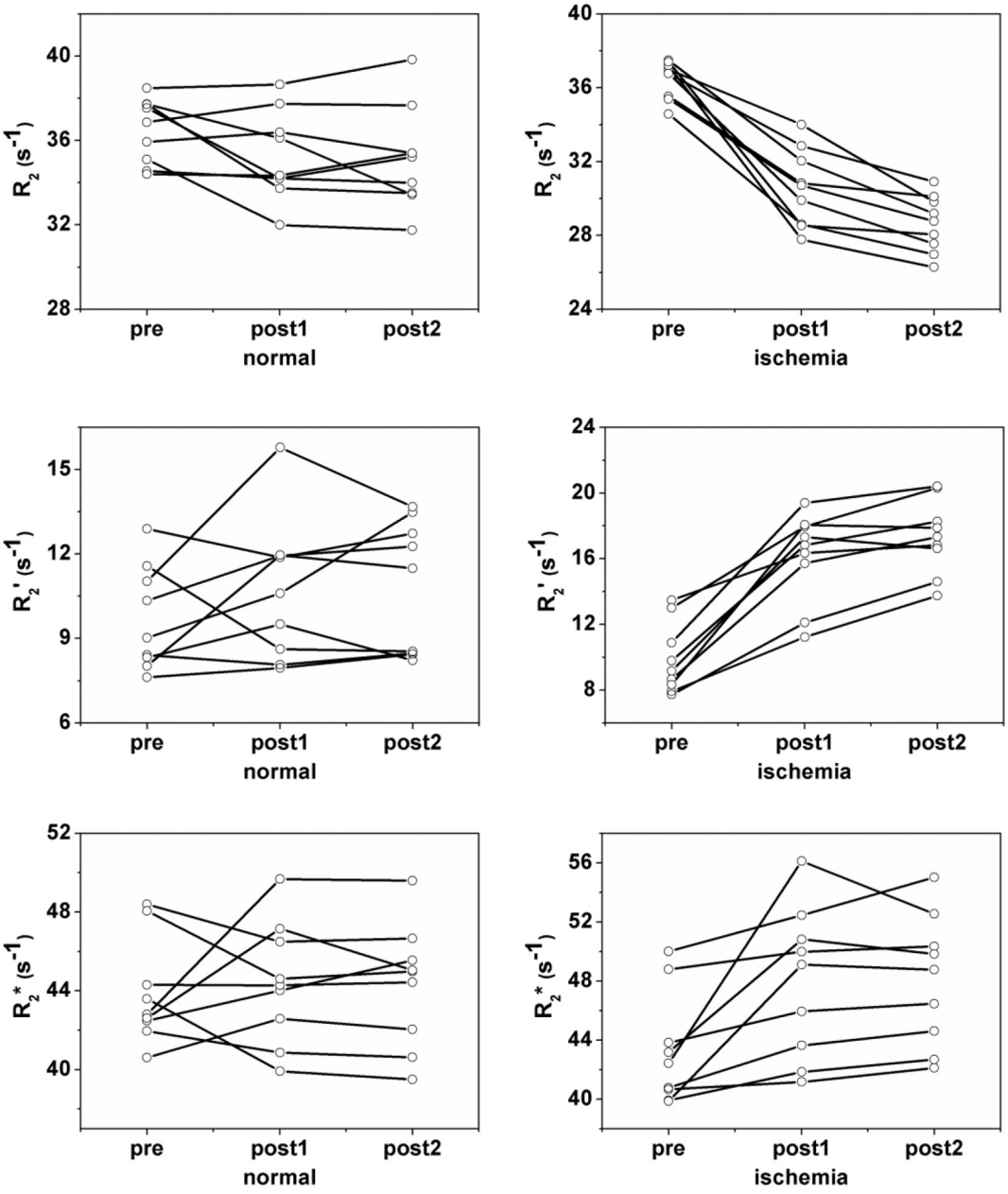

Fig. 5. Inter-subject deviations of R2, R2' and R2* in the left leg muscles of all nine rabbits in the three conditions (pre, post1 and post2). Each polyline represents for one subject.

embolization model to the normal and ischemia legs, the ratios of R2, R2' and R2* between normal and ischemia legs were calculated at three statuses (pre, post1, post2).

3. Results

The MRI data were successfully acquired in all the nine rabbits. The within-session and between-day reproducibility results for R2, R2' and R2* measurements are summarized in Table 1. The within-session CVs of R2, R2s and R2* measurements were 1.57%, 3.33%, and 2.57%, while the between-day CVs were 1.42%, 5.85% and 2.85%, respectively. The reproducibility results supported the feasibility of performing sequential respiratory challenge studies in the same rabbits.

Fig. 3 demonstrates one representative case about the effect of unilateral artery embolization model on T2w image, R2, R2' and R2* maps. It is shown that the R2 decreases obviously from resting state (pre) to the statuses of 1 h (post1) and 2 h (post2) after applying the unilateral artery embolization model. R2' increases significantly from baseline (pre) to the statuses of post1 and post2. Nonetheless, the relative changes in the T2w image and R2* map are much less significant than those in R2 and R2' maps.

The mean and inter-subject deviations of R2, R2' and R2* of all the nine rabbits in the three conditions (pre, post1 and post2) are illustrated in Figs. 4 and 5. In all rabbits, the mean R2 decreases significantly from 36.46 ± 1.03 s^{-1} (pre) to 30.58 ± 2.11 s^{-1} (post1, **P < 0.01) and 28.62 ± 1.53 s^{-1} (post2, **P < 0.01), and the mean R2' goes up markedly from 9.8 ± 2.14 s^{-1} (pre) to 16.10 ± 2.74 s^{-1} (post1, **P < 0.01) and 17.33 ± 2.25 s^{-1} (post2, *P < 0.05). The mean R2* increases from 43.27 ± 3.75 s^{-1} (pre) to 47.90 ± 5.08 s^{-1} (post1, *P < 0.05) and to 48.04 ± 4.42 s^{-1} (post2, NS, P > 0.05).

The mean and ratios of R2, R2' and R2* between normal and ischemia legs of all the nine rabbits in the three conditions (pre, post1 and post2) are illustrated in Figs. 6 and 7.The mean ratio of R2

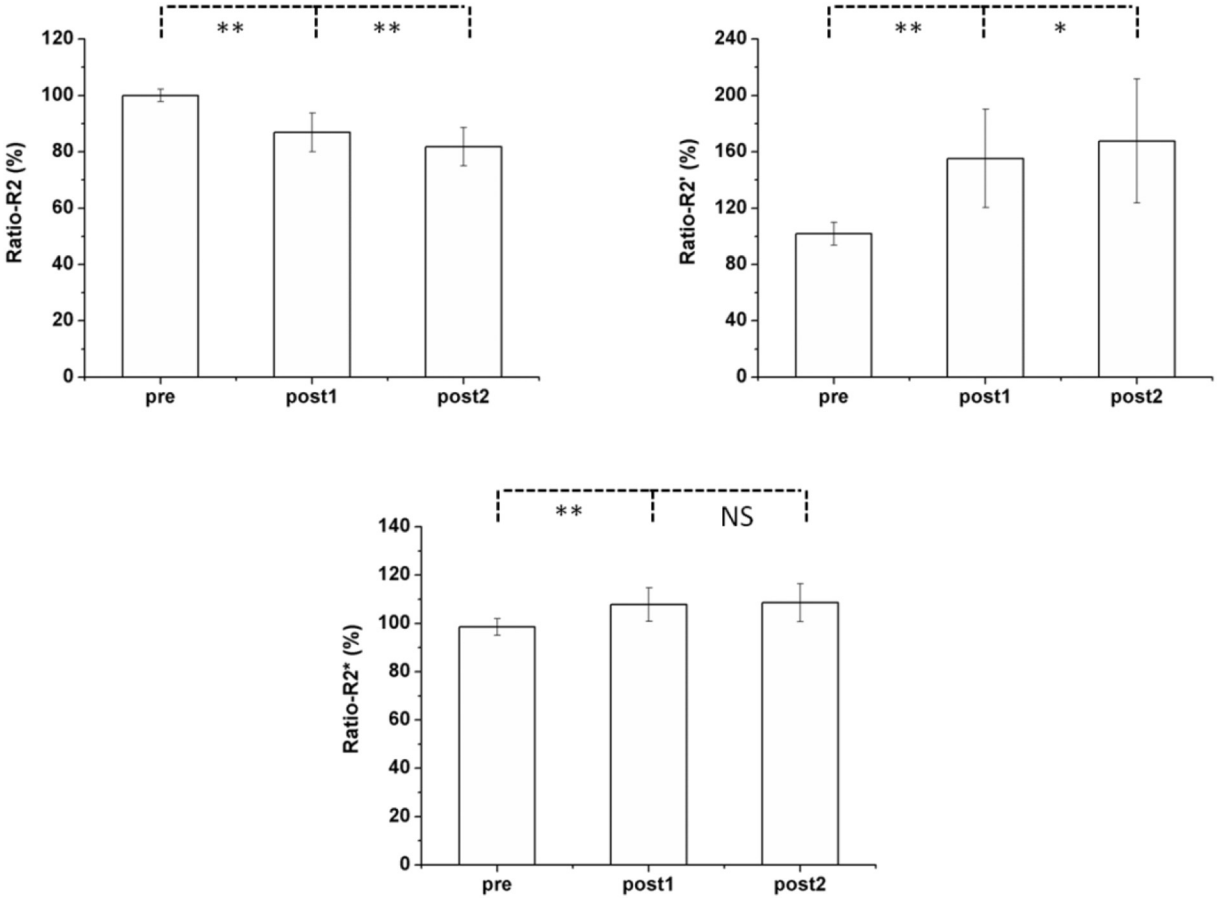

Fig. 6. Average values of the ratios of R2, R2' and R2* between left and right leg muscles of all the nine subjects. *P $<$ 0.05 using paired Student's *t*-test.

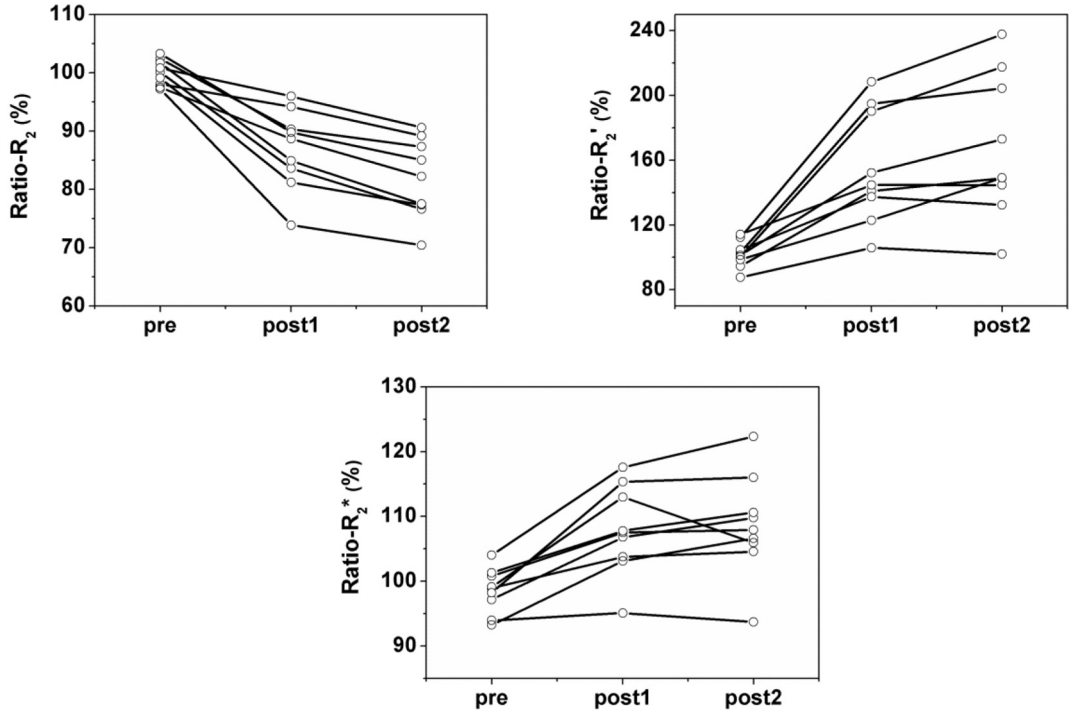

Fig. 7. The ratios of R2, R2' and R2* between normal and ischemia legs of all the nine rabbits in the three conditions (pre, post1 and post2). Each polyline represents for one subject.

decreases significantly from100.01 ± 2.19% (pre) to 86.93 ± 6.85% (post1, **P < 0.01) and 81.79 ± 6.78% (post2, **P < 0.01), and the mean ratio of R2' goes up from 101.79 ± 8.17% (pre) to 155.29 ± 34.87% (post1, **P < 0.01) and 167.70 ± 44.08% (post2, *P < 0.05), while the mean ratio of R2* increases from 98.53 ± 3.44% (pre) to 107.77 ± 6.90% (post1, **P < 0.01) and to 108.61 ± 7.89% (post2, NS,P > 0.05).

4. Discussion

This study demonstrated the feasibility and the necessity of the MEGSE-based simultaneous R2, R2' and R2* measurement approach for the diagnosis of skeletal muscle ischemia and the sensitivity of the R2 and R2' compared with R2* for the evaluation of skeletal muscle oxygenation changes in a rabbit model of unilateral artery embolization. From the results of scan-rescan (within-session and between-day) tests, the R2, R2' and R2* measurements were fairly reproducible. In addition, R2 decreased significantly, and R2' increased significantly, R2 and R2' had a significant opposite trend to the unilateral artery embolization model, which further proved simultaneous R2, R2' and R2* measurement was feasible.

The current measurement of R2, R2' and R2* in rabbit muscle were almost completely absent from the literature. So the resting state muscle R2 at 3T obtained in the present study (36.74 ± 1.09 s^{-1}) were within the normal range, consistent with previous studies in normal human [18,31,32] and rat [33] lower limb muscles. In addition, the decreased tendency of R2 in this unilateral artery embolization model was in accordance with that in a rabbit model of acute ischemia [33].The measurements R2' obtained from rabbit muscle in this paper were also well correlated with the previous reported range of R2' in normal human lower limb muscles [21]. In this unilateral model of vascular embolism, Muscle edema due to acute ischemic embolism caused a significant reduction of R2 [34].The large increase R2' induced by ischemia was also consistent with the decrease of blood flow and the increase of PO_2 which reported in the literature [35,36]. At the same time, the significant increase R2' in this rabbit embolism model was consistent with the significant increase of R2' in the case of lower extremity muscle ischemia caused by the tourniquet compression [18,21], indicating that our experimental results were reasonable. The measurement results showed that this evaluation method could reflect the changes of hypoxia and edema of lower limb muscles before and after embolization.

In this study, we found that R2' and R2 have the opposite significant change trend. We thought the acute ischemia in leg muscles embolization led to the large accumulation of deoxyhemoglobin and then it caused a significant increase in R2' [37].

Acute ischemic embolization can cause muscle edema, and R2 significantly reduced [34]. At the same time, due to R2* = R2 + R2', R2 and R2' were more sensitive to the unilateral leg embolization model in this study compared with R2*. With the above results, we have observed that the pathological changes with the time difference. After embolization, muscle oxygen metabolism changed rapidly, and edema took time to develop. R2' was significantly increased, so the initial R2* was mainly affected by R2'. Later, the embolism model caused the hypoxia and edema, and changes of R2* was caused by the interaction of R2' and R2.

We note that in certain conditions such as muscle infarction in patients with diabetes mellitus, edema and ischemia are often occurred together [38]. However, in some cases such as re-oxygenation, edema and ischemia do not change synchronously. Hypoxia is more sensitive, and edema is delayed compared to ischemia [39]. So R2' changes first and R2 still can reflect the course of the disease. Tissue edema has great damage to the body, so it is more comprehensive to evaluate the two indicators R2 and R2' at the same time, which can better judge the duration and observe the recovery situation of embolism.

Moreover, for some allergic myositis, tissue edema is caused by vascular permeability changes and the first sign is edema and R2 changes first. The time window of edema and hypoxia in different diseases is different and in other words, the sensitivity of R2, R2', R2* is different. Simultaneous R2, R2' and R2* measurement can make the diagnosis of the disease more comprehensive and sensitive. Therefore, the method of simultaneous quantification of R2, R2' and R2* has positive significance for the evaluation of clinical oxygen metabolism and physiological changes in muscles.

Actually, there are some advantages to choose the embolization model rather than ligation model. The internal guide wire enters from the neck and avoids the influence of MRI magnetic susceptibility evaluation while the operation of the leg muscles produces a large amount of blood flow. Moreover, the embolization model can effectively reduce the inauthenticity of ischemia simulation originated form the rapid establishment of collateral circulation by using ligation model [40,41].

Meanwhile, as for the rationality of the MEGSE sequence, for the static muscle imaging, the MEGSE sequence achieves high spatial resolution and could effectively avoid the slice profile mismatch problem between images prior to and after the 180° pulse compared to the GESFIDE and SAGE sequences [19,20], as well as the common EPI artifact to some extent [42].

There exist some limitations in this study. First, the main field and RF field inhomogeneities are likely to cause certain estimation errors in muscle R2, R2' and R2* measurement. To solve this problem, special techniques for B_0 and RF shimming need to be considered in the future. Besides, the MEGSE sequence has a longer imaging time. Because this study is a static muscle measurement, the time resolution is not very high. Second, the muscle images of lower limb were carried out in the resting state, and the interference factors were ignorable, which is similar with previous muscle related oxygen metabolism studies [24,25,43,44],so the mono-exponential model was applicable. Third, the R2* and R2' maps do not appear spatially uniform. The usual argument in favor of the spatially uniform R2', R2* map is the limited compliance of the leg (skin, muscular and connective tissues, and veins). Another explanation may proceed from changes in muscle proton density during reactive hyperemia.

In conclusion, the feasibility and reproducibility of this non-invasive simultaneous R2, R2' and R2* measurement of skeletal muscle based on the MEGSE sequence have been proved in a rabbit model of unilateral artery embolization in our study. This simultaneous R2, R2' and R2* quantification method could be valuable for evaluating skeletal muscle oxygen metabolism.

Acknowledgment

National Natural Science Foundation of China under grant no. 81571666 and 11572003

References

[1] Davies MG. Criticial limb ischemia: epidemiology. Methodist Debakey Cardiovasc J 2012;8(4):10.
[2] Faglia E, Dalla Paola L, Clerici G, Clerissi J, Graziani L, Fusaro M, et al. Peripheral angioplasty as the first-choice revascularization procedure in diabetic patients with critical limb ischemia: prospective study of 993 consecutive patients hospitalized and followed between 1999 and 2003. Eur J Vasc Endovasc Surg 2005;29(6):620–7.
[3] Norgren L, Hiatt WR, Dormandy JA, Nehler MR, Harris KA, Fowkes FGR. Inter-society consensus for the management of peripheral arterial disease (TASC II). J Vasc Surg 2007;45(1):S5–67.
[4] Gu YQ. Determination of amputation level in ischaemic lower limbs. ANZ J Surg 2004;74(1–2):31–3.
[5] Gazzaruso C, Coppola A, Falcone C, Luppi C, Montalcini T, Baffero E, et al. Transcutaneous oxygen tension as a potential predictor of cardiovascular events in type 2 diabetes: comparison with ankle-brachial index. Diabetes Care 2013;36(6):1720–5.
[6] Rudroff T, Weissman JA, Bucci M, Seppänen M, Kaskinoro K, Heinonen I, et al. Positron emission tomography detects greater blood flow and less blood flow heterogeneity in the exercising skeletal muscles of old compared with young men during fatiguing contractions. J Physiol 2014;592(2):337–49.
[7] Kalliokoski KK, Laaksonen MS, Takala TO, Knuuti J, Nuutila P. Muscle oxygen

extraction and perfusion heterogeneity during continuous and intermittent static exercise. J Appl Physiol 2003;94(3):953–8.
[8] Frayne R, Goodyear BG, Dickhoff P, Lauzon ML, Sevick RJ. Magnetic resonance imaging at 3.0 Tesla: challenges and advantages in clinical neurological imaging. Invest Radiol 2003;38(7):385–402.
[9] Partovi S, Karimi S, Jacobi B, Schulte A-C, Aschwanden M, Zipp L, et al. Clinical implications of skeletal muscle blood-oxygenation-level-dependent (BOLD) MRI. Magnetic Resonance Materials in Physics, Biology and Medicine 2012;25(4):251–61.
[10] Kundel HL, Schlakman B, Joseph PM, Fishman JE, Summers R. Water content and NMR relaxation time gradients in the rabbit kidney. Invest Radiol 1986;21(1):12–7.
[11] Alexopoulou E, Stripeli F, Baras P, Seimenis I, Kattamis A, Ladis V, et al. R2 relaxometry with MRI for the quantification of tissue iron overload in β-thalassemic patients. J Magn Reson Imaging 2006;23(2):163–70.
[12] Ni W, Christen T, Zun Z, Zaharchuk G. Comparison of R2′ measurement methods in the normal brain at 3 Tesla. Magn Reson Med 2015;73(3):1228–36.
[13] Prinster A, Pierpaoli C, Turner R, Jezzard P. Simultaneous measurement of ΔR2 and ΔR2* in cat brain during hypoxia and hypercapnia. Neuroimage 1997;6(3):191–200.
[14] Robinson SP, Rijken PF, Howe FA, McSheehy PM, van der Sanden BP, Heerschap A, et al. Tumor vascular architecture and function evaluated by non-invasive susceptibility MRI methods and immunohistochemistry. Journal of Magnetic Resonance Imaging: An Official Journal of the International Society for Magnetic Resonance in Medicine 2003;17(4):445–54.
[15] Wu EX, Tang H, Jensen JH. Applications of ultrasmall superparamagnetic iron oxide contrast agents in the MR study of animal models. NMR in Biomedicine: An International Journal Devoted to the Development and Application of Magnetic Resonance In Vivo 2004;17(7):478–83.
[16] Tropres I, Grimault S, Vaeth A, Grillon E, Julien C, Payen JF, et al. Vessel size imaging. Magnetic Resonance in Medicine: An Official Journal of the International Society for Magnetic Resonance in Medicine 2001;45(3):397–408.
[17] Kiselev VG, Strecker R, Ziyeh S, Speck O, Hennig J. Vessel size imaging in humans. Magnetic Resonance in Medicine: An Official Journal of the International Society for Magnetic Resonance in Medicine 2005;53(3):553–63.
[18] Elder CP, Cook RN, Chance MA, Copenhaver EA, Damon BM. Image-based calculation of perfusion and oxyhemoglobin saturation in skeletal muscle during submaximal isometric contractions. Magn Reson Med 2010;64(3):852–61.
[19] Ma J, Wehrli FW. Method for image-based measurement of the reversible and irreversible contribution to the transverse-relaxation rate. J Magn Reson B 1996;111(1):61–9.
[20] Schmiedeskamp H, Straka M, Bammer R. Compensation of slice profile mismatch in combined spin-and gradient-echo echo-planar imaging pulse sequences. Magn Reson Med 2012;67(2):378–88.
[21] Skinner JT, Robison RK, Elder CP, Newton AT, Damon BM, Quarles CC. Evaluation of a multiple spin-and gradient-echo (SAGE) EPI acquisition with SENSE acceleration: applications for perfusion imaging in and outside the brain. Magn Reson Imaging 2014;32(10):1171–80.
[22] Stokes AM, Skinner JT, Quarles CC. Assessment of a combined spin- and gradient-echo (SAGE) DSC-MRI method for preclinical neuroimaging. Magn Reson Imaging 2014;32(10):1181–90.
[23] Yablonskiy DA, Haacke EM. An MRI method for measuring T2 in the presence of static and RF magnetic field inhomogeneities. Magn Reson Med 1997;37(6):872–6.
[24] Sedlacik J, Reichenbach JR. Validation of quantitative estimation of tissue oxygen extraction fraction and deoxygenated blood volume fraction in phantom and in vivo experiments by using MRI. Magnetic Resonance in Medicine: An Official Journal of the International Society for Magnetic Resonance in Medicine 2010;63(4):910–21.
[25] Wang Z, Xiao J, Xie S, Zhao D, Liu X, Zhang J, et al. MR evaluation of cerebral oxygen metabolism and blood flow in stroke-like episodes of MELAS. J Neurol Sci 2012;323(1–2):173–7.
[26] Sanchez OA, Copenhaver EA, Elder CP, Damon BM. Absence of a significant extravascular contribution to the skeletal muscle BOLD effect at 3 T. Magn Reson Med 2010;64(2):527–35.
[27] Noseworthy MD, Bulte DP, Jeff A. BOLD magnetic resonance imaging of skeletal muscle. Semin Musculoskelet Radiol 2003;7(04):307–16.
[28] Huikuri HV, Kessler KM, Terracall E, Castellanos A, Linnaluoto MK, Myerburg RJ. Reproducibility and circadian rhythm of heart rate variability in healthy subjects. American Journal of Cardiology 1990;65(5):391–3.
[29] Bland JM, Altman DG. Statistics notes: measurement error. Bmj 1996;312(7047):1654.
[30] Razali NM, Wah YB. Power comparisons of shapiro-wilk, kolmogorov-smirnov, lilliefors and Anderson-darling tests. Journal of statistical modeling and analytics 2011;2(1):21–33.
[31] Han E, Gold G, Stainsby J, Wright G, Beaulieu C, Brittain J. In-vivo T1 and T2 measurements of muskuloskeletal tissue at 3T and 1.5 T. Proceedings of the 11th annual meeting of ISMRM. 2003. p. 450.
[32] Psatha M, Wu Z, Gammie FM, Ratkevicius A, Wackerhage H, Lee JH, et al. A longitudinal MRI study of muscle atrophy during lower leg immobilization following ankle fracture. J Magn Reson Imaging 2012;35(3):686–95.
[33] Ha DH, Choi S, Kang EJ, Park HT. Diffusion tensor imaging and T2 mapping in early denervated skeletal muscle in rats. J Magn Reson Imaging 2015;42(3):617–23.
[34] Zhang H, Wang X, Guan M, Li C, Luo L. Skeletal muscle evaluation by MRI in a rabbit model of acute ischaemia. Br J Radiol 2013;86(1026):20120042.
[35] Luo Y, Mohning KM, Hradil VP, Wessale JL, Segreti JA, Nuss ME, et al. Evaluation of tissue perfusion in a rat model of hind-limb muscle ischemia using dynamic contrast-enhanced magnetic resonance imaging. Journal of Magnetic Resonance Imaging: An Official Journal of the International Society for Magnetic Resonance in Medicine 2002;16(3):277–83.
[36] Grinberg OY, Hou H, Grinberg SA, Moodie KL, Demidenko E, Friedman BJ, et al. pO2 and regional blood flow in a rabbit model of limb ischemia. Physiol Meas 2004;25(3):659.
[37] Zhang J, Chen YM, Zhang YT. Blood-oxygenation-level-dependent-(BOLD-) based R2′ MRI study in monkey model of reversible middle cerebral artery occlusion. J Biomed Biotechnol 2011;2011(2):318346.
[38] Chason D, Fleckenstein J, Burns D, Rojas G. Diabetic muscle infarction: radiologic evaluation. Skeletal Radiol 1996;25(2):127–32.
[39] Jelinek JS, Murphey MD, Aboulafia AJ, Dussault RG, Kaplan PA, Snearly WN. Muscle infarction in patients with diabetes mellitus: MR imaging findings. Radiology 1999;211(1):241–7.
[40] de Lussanet QG, van Golde JC, Beets-Tan RG, de Haan MW, Zaar DV, Post MJ, et al. Magnetic resonance angiography of collateral vessel growth in a rabbit femoral artery ligation model. NMR in Biomedicine: An International Journal Devoted to the Development and Application of Magnetic Resonance In vivo 2006;19(1):77–83.
[41] de Lussanet QG, van Golde JC, Beets-Tan RG, Post MJ, Huijberts MS, Schaper NC, et al. Dynamic contrast-enhanced MRI of muscle perfusion combined with MR angiography of collateral artery growth in a femoral artery ligation model. NMR in Biomedicine: An International Journal Devoted to the Development and Application of Magnetic Resonance In vivo 2007;20(8):717–25.
[42] Stables LA, Kennan RP, Gore JC. Asymmetric spin-echo imaging of magnetically inhomogeneous systems: theory, experiment, and numerical studies. Magn Reson Med 1998;40(3):432–42.
[43] An H, Lin W. Quantitative measurements of cerebral blood oxygen saturation using magnetic resonance imaging. Journal of Cerebral Blood Flow & Metabolism 2000;20(8):1225–36.
[44] He X, Yablonskiy DA. Quantitative BOLD: mapping of human cerebral deoxygenated blood volume and oxygen extraction fraction: default state. Magnetic Resonance in Medicine: An Official Journal of the International Society for Magnetic Resonance in Medicine 2007;57(1):115–26.